ELSEVIER

Surface Science 417 (1998) 406–414

surface science

CO_2 chemisorption at Ca and CaO surfaces: a study with MIES, UPS(HeI) and XPS

D. Ochs, B. Braun, W. Maus-Friedrichs, V. Kempter *

Physikalisches Institut der Technischen Universität Clausthal, Leibnizstraße 4, 38678 Clausthal-Zellerfeld, Germany

Received 10 July 1998; accepted for publication 1 September 1998

Abstract

Metastable impact electron spectroscopy (MIES) in combination with UPS(HeI) and X-ray photoelectron spectroscopy was applied to study chemisorption of CO_2 on Ca and CaO films at room temperature. Ca surfaces were prepared by evaporating Ca films (ca 20 nm thickness) on a clean Si(111) surface; information on the topological structure of the Ca film was obtained with scanning tunneling microscopy (STM). CaO films were produced by exposing Ca films to O_2 or N_2O. Ca surfaces exposed to CO_2 become terminated by carbonate complexes (CO_3^{2-}) while features typical for (Ca–O) bonds are detected underneath the surface. A closed carbonate layer forms also when a CaO film is exposed to CO_2. The strong reactivity of the CaO surface against CO_2 is in agreement with recent results of cluster calculations. © 1998 Elsevier Science B.V. All rights reserved.

Keywords: Calcium; Calcium oxide; CO_2; Metastable impact electron spectroscopy (MIES); Photoelectron spectroscopy (UPS(HeI)); Scanning tunneling microscopy (STM)

1. Introduction

The reaction of molecules with oxide surfaces is of great interest for the development of new gas sensors and devices in heterogeneous catalysis. Nevertheless, a fundamental understanding of chemisorption and catalysis is still limited in these cases. So far, the most popular oxide surfaces for gas sensor applications are ZnO and SnO_2 [1]. As far as CaO is concerned, the interaction of SO_2 with CaO(100) has been investigated in some detail with X-ray photoelectron spectroscopy (XPS) under ultrahigh vacuum (UHV) conditions [2,3]. The reactivity of large-area CaO powder with color centers against molecular oxygen was investigated with electron paramagnetic resonance [4]. Cluster calculations modeling the interaction of CO_2 and SO_2 with CaO and MgO were performed by Pacchioni et al. [5,6]. It was found that CO_2 chemisorbs as carbonate molecular ion (CO_3^{2-}) at oxygen sites on both surfaces. The formation of a monodentate carbonate species was predicted. While CO_2 chemisorbs on MgO at low-coordinated oxygen sites only, the carbonate formation occurs also at regular oxygen sites on CaO. The prediction made for MgO is supported by our previous measurements [7,8].

In this article we study the chemisorption of CO_2 on CaO surfaces applying essentially the same strategy as in our previous studies concerned with the chemisorption of CO_2 on MgO [7,8]. At first, we describe ways to produce CaO films starting with a Ca surface. Then, we study the interaction

* Corresponding author. Fax: +49 5323 723600;
e-mail: volker.kempter@tu-clausthal.de

0039-6028/98/$ – see front matter
PII: S0039-6028(98)00721-3

of the Ca and CaO films with CO_2. We characterize the electronic structure of Ca and CaO surfaces, before and after exposure to CO_2, by combining metastable impact electron spectroscopy (MIES), photoelectron spectroscopy UPS(HeI) and XPS. The identification of the CO_2 induced features is accomplished from a comparison with the spectral features developed when CO_2 interacts with Ca surfaces. This task is facilitated by the information already available on the CO_2 interaction with other metal surfaces [9,10]. Information on the topology of the Ca surface comes from scanning tunneling microscopy (STM).

2. Experimental

The experiment was carried out in an UHV system (base pressure $<2\times10^{-10}$ Torr) consisting of a chamber for electron spectroscopies and another one for sample treatment [7,11,12]. The former one is equipped with facilities for XPS, low energy electron diffraction (LEED) and Auger electron spectroscopy (AES) and a cold-cathode gas discharge source for the production of metastable He*($2^3S/2^1S$) ($E^*=19.8/20.6$ eV) atoms with thermal kinetic energies as a source for MIES and HeI photons ($E^*=21.2$ eV) as a source for UPS [11] (and references cited therein). The triplet-to-singlet ratio has been measured by He*–Ar impact as 7:1. Metastable and photon contributions within the beam are separated by means of a time-of-flight technique using a mechanical chopper in combination with a double counter system allowing to measure MIES and UPS quasi-simultaneously. All electron energy spectra were acquired with the incident photon/metastable beams under 45° with respect to surface normal in the constant pass energy mode using a hemispherical analyzer with an acceptance angle of 8° (FWHM); the binding energies are referenced to the Fermi level E_F. By biasing the sample with respect to the analyzer (50 eV) the variation of the surface work function with exposure can be determined directly from the high binding energy cutoff of the electron spectra. For binding energies larger than ca 10 eV both the UPS and the MIES spectra appear to be influenced by secondary electrons; this part of the spectra will not be discussed in the following.

The STM apparatus consists of a commercial Perkin–Elmer chamber (base pressure $<1\times10^{-10}$ Torr) equipped with an Omicron Micro-STM [13]. It is furthermore equipped with a cylindrical mirror analyzer (CMA) to perform AES. The target is cleaned in a preparation stage in order to prevent an eventual contamination of the STM. The STM images were taken in the constant current topography (CCT) mode. The bias voltage given with the images corresponds to the target potential. The STM tip is fixed at zero potential. The calibration of the scanner z-coordinate is known from a previous study [13]. The n-doped Si(111) substrate was prepared from commercial wafers. They were cleaned by electron bombardment, heating to ca 1200°C for several minutes with subsequent cooling down to a temperature of ca 600°C within 10 min. After this procedure the silicon substrates showed the Si(111)-(7×7) reconstruction both in LEED and STM. Ca layers were produced by evaporating calcium from a commercial Knudsen cell in the MIES apparatus and a home-built evaporator in the STM chamber. During the evaporation of Ca the pressure never rose beyond 3×10^{-9} mbar. All measurements are performed at room temperature.

3. Results

3.1. Characterization of Ca and CaO films

Fig. 1 shows the STM image of the Si(111) surface covered by a closed Ca film (total thickness >20 nm). The surface is terminated by three-dimensional islands. Their lateral size is between 50 and 100 nm; their height is ca 5 nm, typically. The step height between each two terraces of the hexagonal islands is 2.64 ± 0.2 Å, which is close to half of the Ca(fcc) lattice constant (2.79 Å [14]). Furthermore, most islands are aligned relative to each other. Although atomic resolution could not be achieved, our findings appear to suggest that the islands consist of well ordered Ca atoms.

The MIES spectra of Ca films on Si(111) exposed to oxygen are presented in Fig. 2. The

Fig. 1. 300 nm × 350 nm STM image of the Ca film on Si(111); max. height difference, 10 nm; bias voltage, −2 eV; tunneling current, 1.2 nA.

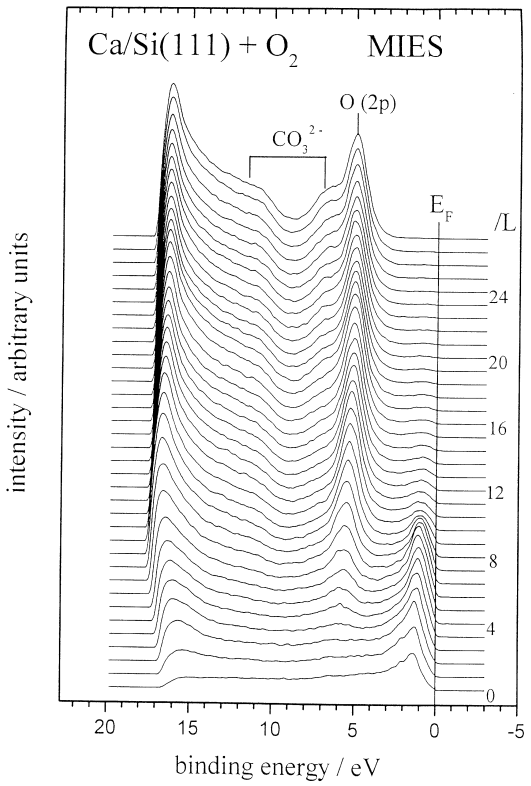

Fig. 2. MIES spectra of Ca film (thickness >20 nm) on Si(111) exposed to O_2.

bottom spectrum applies to the clean Ca film and shows a well-developed Fermi edge. This is characteristic for spectra caused by Auger deexcitation. Hereby, an electron from the uppermost occupied Ca band fills the He 1s hole of the probe atom while the He 2s electron is emitted, carrying the excess energy [15,16]. The work function of the Ca film, derived from the low energy onset of the bottom MIES spectrum, is 3.2 ± 0.2 eV; the value for Ca(100) is 2.8 eV [15].

The presence of oxygen at the surface manifests itself in two respects:

(1) in the development of a new peak at ca $E_B = 5.5$ eV; and
(2) in the spectral changes and, finally, the disappearance of the structure close to E_F which is representative for the metallic part of the surface density of states (SDOS).

By comparison with the corresponding structure observed during the oxygen exposure of Mg films [8,12] we attribute the feature seen at ca $E_B = 5.5$ eV to the ionization of O 2p of oxygen atoms chemisorbed at the Ca surface.

The spectral changes upon oxygen exposure observed in the metallic part of the SDOS can probably be understood as follows: in the initial stage of the exposure the s-part of the SDOS becomes preferentially involved in the bonding of the oxygen, and its contribution to the Ca charge density is strongly reduced. Therefore, MIES samples the higher angular moment components of the metallic part of the surface charge density which are less involved in (Ca–O) bonds. In particular, the p- and e_g-part of the DOS is strongly peaked at E_F [17], and may therefore be responsible for the narrowing of the peak seen near E_F.

The formation of a $He^-*(1s2s^2)$ species and its decay by autodetachment offers a second possi-

bility to explain the observed increase in intensity near E_F [18]. However, the work function needs to decrease to values below ca 2.2 eV upon exposure to O_2 or CO_2 for efficient formation of He^-* [18]. This is not the case for Ca exposed to either O_2 or CO_2, and for this reason we expect at most a small contribution of the autodetachment process to the spectra of Figs. 2 and 5.

The work function decreases during the initial stage of the exposure and reaches its minimum ca 10 L (1 L = 10^{-6} Torr s). Around 20 L the metallic part of the SDOS has virtually disappeared. The intensity of the O 2p feature saturates ca 16 L, and the work function has adopted its final value of ca 3 eV.

The energy difference between the top of the valence band and the Fermi level E_F gives the lower part of the bandgap of the insulating layer. For defect free bulk insulators the Fermi level would be located in the middle of the band gap. Under this assumption a bandgap width of 7 ± 0.2 eV is derived from the top spectra of Figs. 2 and 3 (6.9 eV for the CaO bulk [1]).

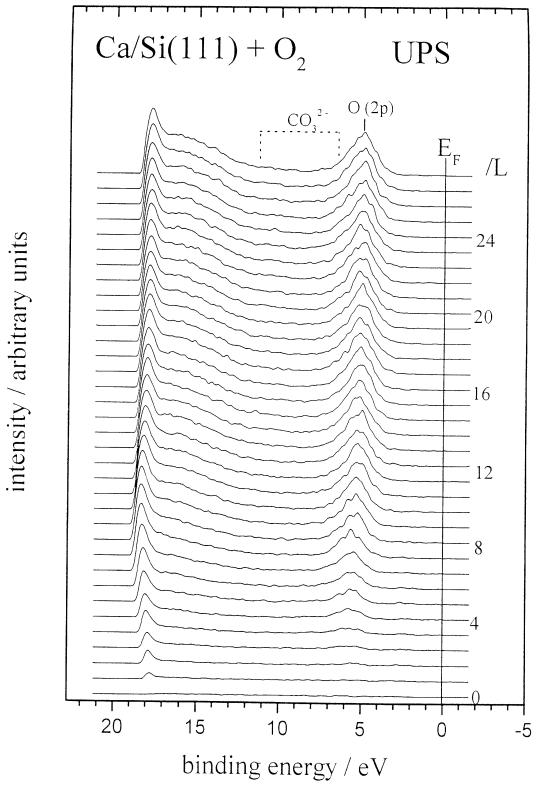

Fig. 3. UPS spectra of Ca film (thickness >20 nm) on Si(111) exposed to O_2.

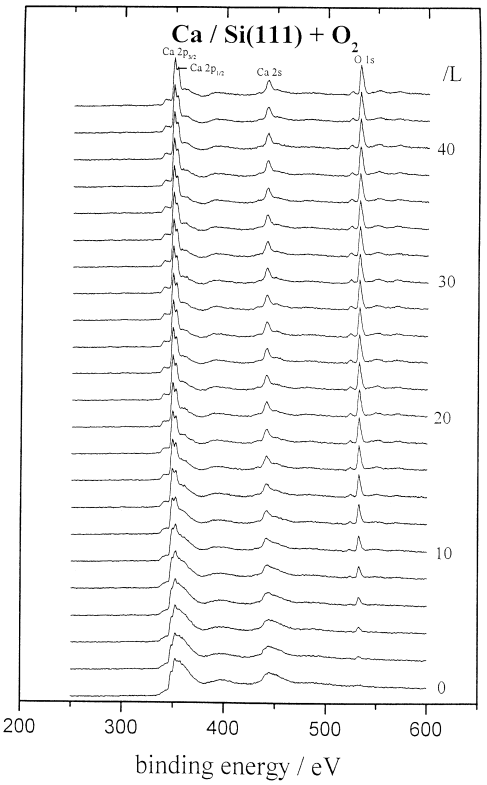

Fig. 4. XPS spectra of Ca film (thickness >20 nm) on Si(111) exposed to O_2.

The distance from E_F to the vacuum level, the work function of the insulating film, is taken from the onset of the spectra at large binding energies. Thus, the distance from the top of the valence band to the vacuum level, as derived from both the MIES and UPS results, is 6.2 eV.

Two additional features, labeled CO_3^{2-}, appear at $E_B = 7$; 11.8 eV which can be attributed to a small surface contamination by carbonate ions (see Section 3.2). We cannot exclude that the presence of an OH-species at the surface also contributes to these features [19].

The UPS results of Fig. 3 are rather insensitive to the metallic part of the DOS, but they confirm the presence of chemisorbed oxygen by the occur-

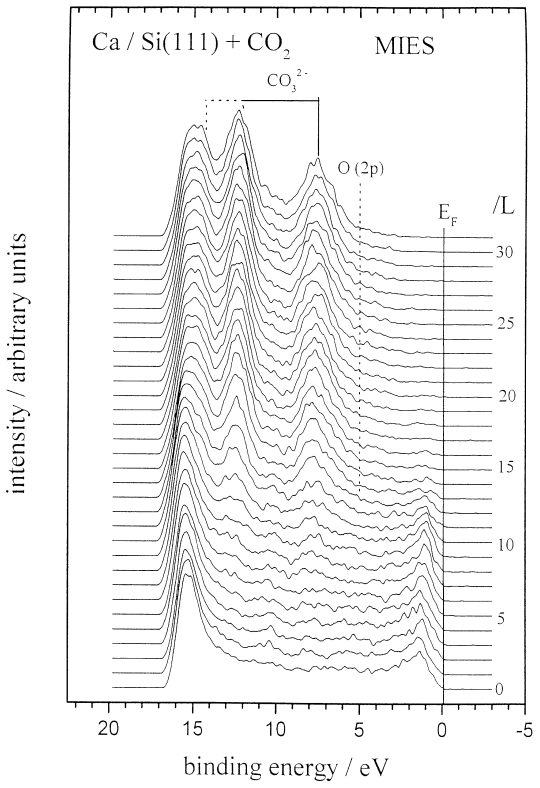

Fig. 5. MIES spectra of Ca film (thickness >20 nm) on Si(111) exposed to CO_2.

rence of the peak at $E_B = 5.5$ eV that we attribute to the ionization of O 2p. No features develop in UPS at the positions where carbonate features are expected (see dashed lines) supporting the assumption of the surface origin of the additional species seen with MIES.

Fig. 4 shows the XPS spectra collected for oxygen exposures up to 44 L. The spectrum of the clean Ca film displays two broad structures at $E_B = 360$; 450 eV which can be assigned to the ionization of the Ca 2p and Ca 2s orbitals. Both structures narrow considerably upon oxygen exposure: the Ca 2p peak develops into a double-peak structure at $E_B = 348.6$; 352.0 eV which is caused by the ionization of the two fine structure components Ca $2p_{3/2}$ and Ca $2p_{1/2}$. The Ca 2s structure develops into a peak centered at 441 eV. A new peak appears at $E_B = 532.2$ eV, due to ionization of O 1s, displaying a linear rise in intensity up to ca 20 L.

We propose the following interpretation to the oxygen-induced changes:

- The broad structures, assigned to the ionization of the Ca 2p and Ca 2s orbitals, are caused by "shake-up" processes into empty metallic states still available in the initial stage of the oxygen exposure. These processes produce shoulders towards higher binding energies with respect to the main peaks [20]. The states responsible for the "shake-up" processes are not available anymore after the bandgap formation has occurred in the near-surface region.
- The O 1s feature at 532.2 eV saturates at ca 22 L while the O 2p signal in UPS reaches already saturation at ca 18 L [21]. This, together with the fact that no metallic features can be seen beyond ca 20 L, suggest that an insulating film has formed.
- XPS spectra obtained by us from a CaO(100) single crystal (not shown here) are practically identical to the saturation spectra presented in Fig. 4, both as far as the position of the peaks and their relative intensities are concerned [21]. This leads us to the conclusion that indeed a stoichiometric CaO film (thickness >10 nm) has formed.

We can compare our MIES and UPS results to ab initio results obtained by applying the full potential photoemission theory to CaO(100) [22]. The agreement with the full potential angle-resolved valence band spectra in the ΓXWK emission plane for unpolarized HeII radiation is rather good, in particular as far as the width and shape of the valence band emission are concerned. This suggests that final state effects may be neglected and that our MIES (UPS) results do mainly represent the SDOS (DOS) of the valence band states, respectively. When Ca films on Si(111) are exposed to N_2O molecules, the oxygen-induced changes and the equilibrium spectra are, within the accuracy of our results, identical to those presented in Figs. 2–4 although a larger exposure (ca 100 L) is required to reach this stage [21,23]. This finding is compatible with the assumption that the N_2O molecules dissociate when interacting with the surface. While the N_2 fragments leave the

surface, the oxygen atoms form (Ca–O) bonds. Ultimately, the film turns into a CaO layer, just as for O_2 exposure. Again a small surface contamination with carbonate ions is detected with MIES.

Equilibrium spectra identical to those obtained with O_2 and N_2O can also be obtained from the evaporation of Ca in an oxygen ambient atmosphere [21,23]. The coincidence of the equilibrium spectra from three different methods is further evidence that indeed a CaO film is produced in all three cases.

3.2. Ca films exposed to CO_2

The MIES and UPS(HeI) results obtained during the CO_2 exposure of a Ca film (>20 nm thick) on Si(111) are presented in Figs. 5 and 6; a small oxygen contamination is seen in the UPS, but not in the MIES spectra. The exposure dependence differs considerably from that for O_2 and N_2O. Moreover, the MIES and UPS results display considerable differences among each other. Peaks, labeled CO_3^{2-}, appear in the MIES spectra at $E_B = 7.6$; 12.2 eV, and possibly at 14.5 eV. They are also seen with UPS where they are superimposed by the feature O 2p. The identification of the spectral features follows from photoelectron spectroscopy results for $CaCO_3$ bulk samples [24] and from our previous work dealing with the CO_2 interaction with Mg and MgO surfaces where the same features were seen [7,8]. They are due to the ionization of a carbonate (CO_3^{2-}) species, and can be assigned to the MOs ($1a_2'$; $1e'$; $4e'$) (7.6 eV), ($3e'$;$1a_2'$) (12.2 eV) and ($4a_1'$) (14.5 eV) [24]. The emission from CO_3^{2-} increases up to ca 20 L and, thereafter, remains almost unchanged.

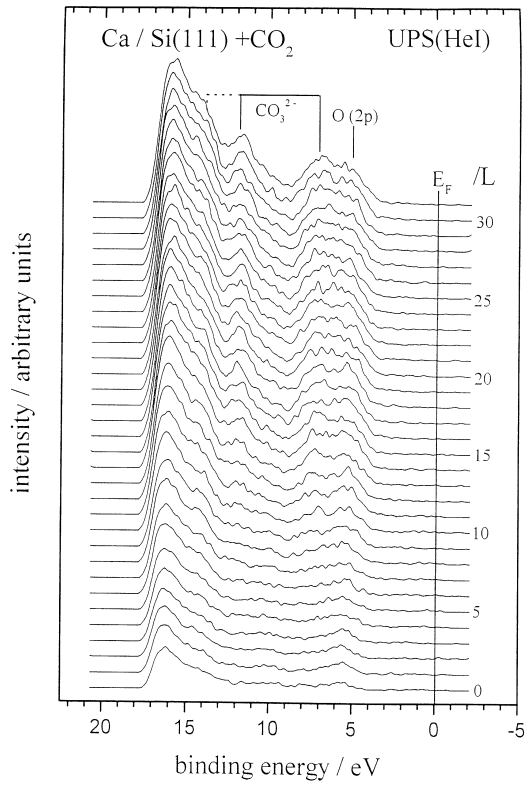

Fig. 6. UPS spectra of Ca film (thickness >20 nm) on Si(111) exposed to CO_2.

The UPS spectra are more complicated: besides the emission from CO_3^{2-} which is also seen, the structure labeled O 2p is present. By comparison with the O_2 and N_2O results we assign it to the ionization of O 2p from atomic oxygen species involved in (Ca–O) bonds. It is remarkable that O 2p is seen in UPS before the carbonate emission becomes visible in MIES.

The XPS spectra of Fig. 7 can be analyzed along the same lines as those of Fig. 4. The metallic character of the surface has disappeared above ca 32 L as judged from the absence of the shake up features. The O 1s peak is split into two components at 532 and 536 eV which we attribute, by comparison with Fig. 4, to oxygen in (Ca–O) bonds (532 eV) and in carbonate complexes (536 eV); the exposure dependence of the peak intensities is more complicated than in Fig. 4.

For reviews of the surface chemistry of CO_2 the reader is referred to Refs [9,10]. Our spectroscopic results obtained with MIES, UPS and XPS show that, as in the case of Mg [9,10], the CO_2 adsorption is dissociative. The presence of oxygen atoms at the surface promotes the bonding of CO_2 as carbonate species. The MIES data, in particular, show that the carbonate and oxide species have rather different distributions in the near-surface regions with the carbonate being confined to the topmost layer and the oxide present as an underlayer. The present results are compatible with the following scenario for the interaction of CO_2

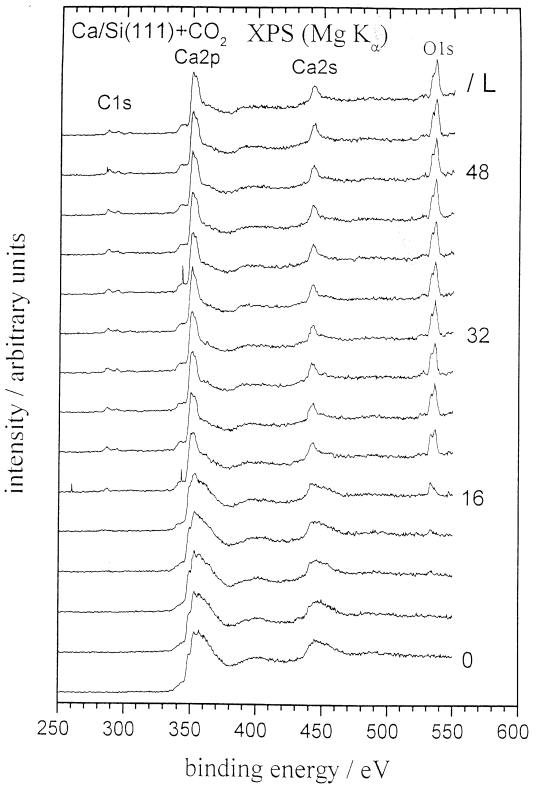

Fig. 7. XPS spectra of Ca film (thickness >20 nm) on Si(111) exposed to CO_2.

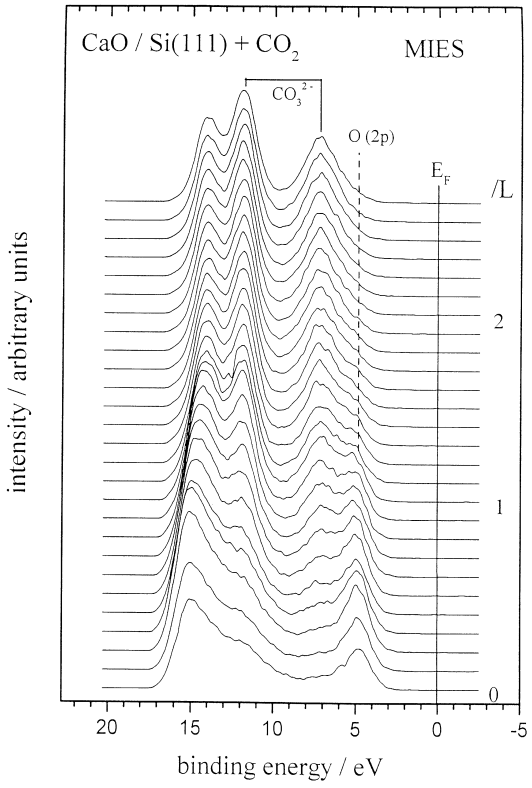

Fig. 8. MIES spectra of CaO film (thickness >10 nm) on Si(111) exposed to CO_2.

with Ca surfaces first proposed for the interaction of CO_2 with Mg surfaces [25] (see also our previous results for Mg [7,8]):

(1) the CO_2 molecules dissociate on the surface; in this way (Ca–O) bonds are formed; and
(2) additional CO_2 can react with surface oxygen which leads to the CO_3^{2-} termination of the surface.

It is remarkable that, despite the carbonate termination of the surface, a CaO film with >10 nm thickness forms. Additional spectroscopic studies at lower surface temperatures would be desirable for clarification of the details of the reaction dynamics.

3.3. CaO exposed to CO_2

Fig. 8 shows the MIES results for CO_2 exposure of CaO films on Si(111). We start with a CaO film prepared along the lines described in Section 3.2. The film thickness is ca 10 nm. The MIES spectra of the "as prepared" CaO surface display the density of states in the uppermost filled valence band discussed in the previous sections. After CO_2 exposure the two features labeled CO_3^{2-} emerge at $E_B = 7.2$; 12.0 eV. They are due to the ionization of a surface carbonate species (see Section 3.2), and are also seen, although only weakly, when exposing MgO surfaces to CO_2 [7,8]. After an exposure of 2 L the two features have developed into strong peaks, and very little contribution from O 2p ionization can be seen in the spectra. In saturation the spectra become very similar to those obtained when exposing the Ca film to oxygen (Section 3.1).

In Fig. 9 the corresponding UPS measurements are shown. Structure CO_3^{2-} superimposes the O(2p) peak located at ca 5 eV. Under saturation

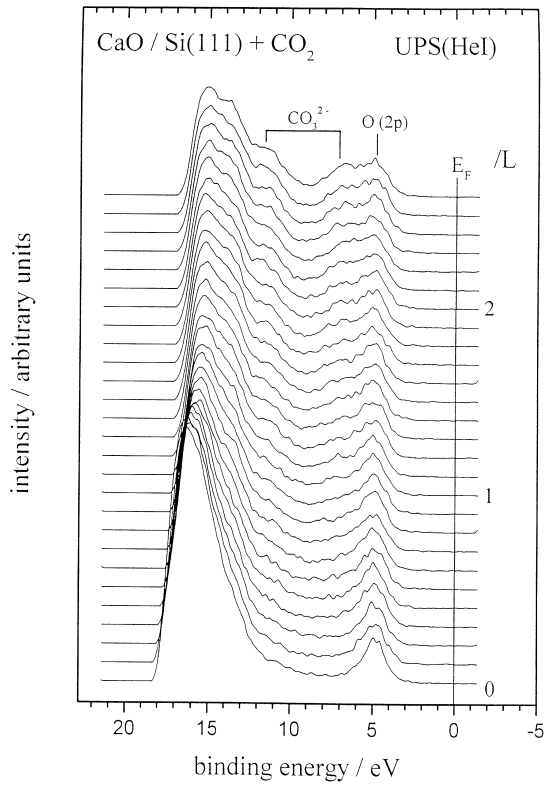

Fig. 9. UPS spectra of CaO film (thickness >10 nm) on Si(111) exposed to CO_2.

conditions, the structures O 2p and CO_3^{2-} are of comparable intensity. The spectrum becomes then, as for MIES, very similar to that obtained from exposing the Ca film to oxygen (Section 3.1).

Obviously, a closed CO_3^{2-} layer forms on top of the CaO surface. For MgO surfaces exposed to CO_2 the carbonate features at ca $E_B = 7.6$; 12.2 eV appear too, but with much less intensity [7,8]; in saturation their intensity is about two orders of magnitude smaller.

The chemisorption of CO_2 on MgO and CaO was studied theoretically by performing cluster calculations [5,6]; it is found that on MgO CO_2 can chemisorb at fourfold-coordinated O_{4c}^{2-} step sites. It forms a chemisorbed complex whose geometry resembles that of a monodentate carbonate CO_3^{2-} species. The (O–C–O) unit is considerably distorted from the gas phase linear structure: the (C–O) distance is stretched by 0.06 Å, and the (O–C–O) angle is reduced to ca 130°. The interaction involves charge transfer from the uppermost filled O 2p states at surface ions into the vacant π_u^* MO of CO_2. This charge transfer occurs more easily at a low coordinated defect site, O_{4c}^{2-}, than at regular O_{5c}^{2-} sites: at fourfold-coordinated O_{4c}^{2-} step sites the electrons are less strongly bound, and charge can flow to the adsorbed CO_2.

A dramatic difference was predicted for the reactivity of CaO against CO_2: strong adsorption with a binding energy of ca 1 eV takes place at regular O_{5c}^{2-} sites of the surface. The surface complex is not very different from that formed in the case of MgO at low-coordinated O_{4c}^{2-} defect sites. According to Refs [5,6] the strongly different reactivity of the two oxide surfaces can be ascribed to the different Madelung potentials of the two surfaces. This has two important consequences:

(1) the electron cloud of the O_2^- anions in CaO is spatially more diffuse than in MgO and can overlap more efficiently with the unoccupied π_u^* of the incoming CO_2 molecules; and
(2) the HOMO donor orbital O_2^- lies at ca 11 eV in MgO, but at ca 8.5 eV in CaO.

Thus, charge can be donated to the adsorbing CO_2 molecule at a lower cost in CaO than in MgO. As a consequence, the Madelung potential at a regular O_{5c}^{2-} site of the CaO surface is intermediate between that of a step and a corner defect site of MgO.

The numerical results find support by our results for the CO_2 chemisorption on MgO [7,8] and the present work on CaO: for MgO a saturation carbonate coverage of the order of only 1% of the number of available oxygen sites is obtained at room temperature. On the contrary, the number of carbonate complexes is about two orders of magnitude larger for CaO.

No chemisorbed species, as f.i. $CO_2^{\delta-}$ and $O_2^{\delta-}$, could be detected with MIES when CaO films, prepared as described in Section 3.2, were exposed to CO and O_2, respectively [23].

4. Summary

Ca films were exposed to O_2 and N_2O molecules at room temperature in order to produce a CaO

film. Information on the topological structure of the Ca film was obtained with STM. The electronic structure of the Ca film and the structural changes taking place during gas exposure were studied with the electron spectroscopic techniques MIES, UPS(HeI) and XPS. The results indicate that a stoichiometric CaO film, >10 nm thick, can be produced in this way.

Ca exposed to CO_2 at room temperature develops spectral features which arise from the ionization of the $(1a_2'; 1e'; 4e')$, $(3e'; 1a_2')$ and $(4a_1')$ molecular orbitals of the carbonate molecule ion (CO_3^{2-}). UPS shows the same features, but superimposed by a peak which is assigned to the ionization of O 2p. The results support the following sequence of processes for the interaction of CO_2 with Ca:

(1) the CO_2 dissociates upon interacting with the surface whereby (Ca–O) bonds are formed; and
(2) additional CO_2 reacts with surface oxygen which leads to CO_2 chemisorption in form of CO_3^{2-}.

This mechanism is the same as proposed for the CO_2 interaction with Mg surfaces [7,8,25].

A closed carbonate layer forms when a CaO film is exposed to CO_2 at room temperature. This is in contrast to MgO where CO_2 chemisorbs at low-coordinated oxygen sites only [7,8]. According to Refs [5,6] the strongly different reactivity of the two surfaces can be attributed to the different Madelung potentials with the consequence that charge donation to the chemisorbing CO_2 can occur at a lower cost in CaO than in MgO.

Acknowledgements

Financial assistance came from the DAAD/BC project ARC 313-ARC-XI-97/51. The authors acknowledge fruitful discussions with A. Shluger and L. Kantorovich (University College London).

References

[1] V.E. Henrich, P.A. Cox, The Surface Science of Metal Oxides, Cambridge University Press, Cambridge, 1994.
[2] Y.C. Lee, P.A. Montano, J.M. Cook, Surf. Sci. 143 (1984) 423.
[3] C.D. Stinespring, J.M. Cook, J. Electron Spectrosc. Relat. Phenom. 32 (1983) 113.
[4] M. Chiesa, M.C. Paganini, E. Giamello, Langmuir 13 (1997) 5306.
[5] G. Pacchioni, Surf. Sci. 281 (1993) 207.
[6] G. Pacchioni, J.M. Ricart, F. Illas, J. Am. Chem. Soc. 116 (1994) 10152.
[7] D. Ochs, M. Brause, B. Braun, W. Maus-Friedrichs, V. Kempter, Surf. Sci. 397 (1998) 184.
[8] D. Ochs, M. Brause, W. Maus-Friedrichs, V. Kempter, J. Electron Spectrosc. Relat. Phenom. 88 (1998) 757.
[9] F. Solymosi, J. Molec. Cat. 65 (1991) 337.
[10] H.-J. Freund, M.W. Roberts, Surf. Sci. Rep. 25 (1996) 225; J. Electron. Spectrosc. Relat. Phenom. 18 (1980) 23.
[11] W. Maus-Friedrichs, M. Wehrhahn, S. Dieckhoff, V. Kempter, Surf. Sci. 237 (1990) 257.
[12] D. Ochs, W. Maus-Friedrichs, M. Brause, J. Günster, V. Kempter, V. Puchin, A. Shluger, L. Kantorovich, Surf. Sci. 365 (1996) 557.
[13] J. Hauschild, H.J. Elmers, U. Gradmann, Phys. Rev. B 57 (1998) R677.
[14] R.W.G. Wyckoff, Crystal Structures, Wiley, 1965.
[15] G. Ertl, J. Küppers, Low Energy Electrons and Surface Chemistry, VCH, Weinheim, Berlin, 1985.
[16] V. Kempter, Comments on Atomic and Molecular Processes 34 (1998) 11.
[17] D.A. Papaconstantopoulos, Handbook of the Band Structure of Elemental Solids, Plenum Press, New York, 1986.
[18] J. Günster, Th. Mayer, V. Kempter, Surf. Sci. 359 (1996) 155.
[19] J. Günster, G. Liu, V. Kempter, D.W. Goodman, J. Vac. Sci. Technol. A 16 (1998) 996.
[20] D. Briggs, M.P. Seah (Eds.), Practical Surface Analysis by Auger and X-ray Photoelectron Spectroscopy, Wiley, Chichester, 1983.
[21] B. Braun, Diploma Thesis, TU Clausthal, unpublished.
[22] M. Grass, J. Braun, G. Borstel, Surf. Sci. 334 (1995) 215.
[23] D. Ochs, Doctoral Thesis, TU Clausthal, 1998.
[24] E. Tegeler, N. Kosuch, G. Wiech, A. Faessler, J. Electron Spectrosc. Relat. Phenom. 18 (1980) 23.
[25] S. Campbell, P. Hollins, E. McCash, M.W. Roberts, J. Electron Spectrosc. Relat. Phenom. 145 (1986) 145.